PERGAMON

International Journal of Heat and Mass Transfer 44 (2001) 811–826

International Journal of HEAT and MASS TRANSFER

www.elsevier.com/locate/ijhmt

Evaporation of water by free convection in a vertical channel including effects of wall radiative properties

C. Debbissi[a], J. Orfi[b], S. Ben Nasrallah[c,*]

[a]*Institut Préparatoire aux Etudes d'Ingénieurs de Monastir, Avenue Ibn Eljazzar, Monastir 5019, Tunisia*
[b]*Département de Physique, Faculté des Sciences de Monastir, Avenue Ibn Eljazzar, Monastir 5019, Tunisia*
[c]*Département d'Energétique, Ecole Nationale d'Ingénieurs de Monastir, Avenue Ibn Eljazzar, Monastir 5019, Tunisia*

Received 4 May 1999; received in revised form 20 March 2000

Abstract

The present study consists of a numerical investigation of coupled heat and mass transfers by natural convection during water evaporation in a vertical channel heated symmetrically by a uniform flux density by taking into account radiative heat transfer between the plates. The governing equations are solved numerically by a finite difference method. The spatial profiles of velocity, temperature and moisture are presented. The effect of ambient conditions, channel width and walls radiation are also analysed in this study.

1. Introduction

Evaporation of liquids by free convection driven by thermal and mass buoyancy forces is frequently encountered in engineering processes and natural environments. The simultaneous diffusion of metabolic heat and perspiration in controlling our body temperature is an example of such flow. Distillation of a volatile component from a mixture with involatiles is one among several other industrial applications where combined heat and mass transfer process takes place.

Steady natural convection flows induced by the buoyancy forces of thermal diffusion in vertical ducts have been extensively investigated [1–4]. Aung and Worku [1] studied the flow reversal in a vertical channel with asymmetric wall temperatures. It has been shown [2] that when the wall temperatures are unequal, a reversal flow situation occurs if the magnitude of the buoyancy force (parameter Gr/Re) exceeds a certain threshold value.

The effects of mass diffusion on natural thermal convection flow have been widely investigated for vertical, horizontal and recently inclined flat plates [5–8]. Yan and Soong [7] studied numerically the evaporation of water vapour along an inclined heated plate. The influences of the inclined angle, the wall heating flux, the inlet film thickness and the free stream velocity on the momentum, heat and mass transfer in the system are clarified. Mammou et al. [8] presented a numerical study of the laminar heat and mass transfer from an inclined flat plate with a dry zone inserted between two wet zones. They concluded that the inclination angle has a small influence on the local Nusselt and Sherwood numbers. On the other hand, the velocity, temperature and vapour concentration profiles are

* Corresponding author. Tel.: +216-3-500511; fax: +216-3-500514.

E-mail address: sassi.bennasrallah@enim.rnu.tn (S.B. Nasrallah).

0017-9310/01/$ - see front matter
PII: S0017-9310(00)00125-3

Nomenclature

C	mass fraction of water vapour
c_p	specific heat (J kg^{-1} K^{-1})
c_{pa}	specific heat for air (J kg^{-1} K^{-1})
c_{pv}	specific heat for water vapour (J kg^{-1} K^{-1})
d	half channel width (m)
D	mass diffusivity (m^2 s^{-1})
e	plates emissivity
$F_{i\to k}$	diffuse view factors between infinitesimal areas i and k
g	gravitational acceleration (m s^{-2})
Gr_M	Grashof number ($g\beta qH^4/\nu_0^2\lambda$)
H	channel length (m)
i	grid point index number in the flow direction
I	upper grid point index number in the x direction
j	grid point index number in the transverse direction
J	upper grid point index number in the y direction
Lv	latent heat of evaporation (J kg^{-1})
$\dot{m}$	evaporating mass flow (kg s^{-1} m^{-2})
M_a	molecular weight of air (kg mol^{-1})
M_v	molar mass of vapour (kg mol^{-1})
Nus	interfacial Nusselt number for sensible heat transfer $(-x\lambda(\partial T/\partial y\|_{y=2d})1/T(x, 2d) - T_0)$
O_1	up channel opening
O_2	down channel opening
p	pressure of the moist air in the channel (N m^{-2})
P	motion pressure (dynamic pressure) (N m^{-2})
p_v	partial pressure of vapour (N m^{-2})
p_{vs}	partial pressure of saturated vapour (N m^{-2})
p_0	ambient pressure (N m^{-2})
q	external heat flux (W m^{-2}) ($q = q_1 + q_2$)
q_l	interfacial latent heat flux (W m^{-2})
q_o	plate radiosity (W m^{-2})
q_r	local net radiative heat flux leaving plates (W m^{-2})
q_s	interfacial sensible heat flux (W m^{-2})
T	absolute temperature (K)
u	axial velocity (m s^{-1})
v	transverse velocity (m s^{-1})
w	relative humidity (p_v/p_{vs}) (%)
x	coordinate in the axial direction (m)
y	coordinate in the transverse direction (m)

Greek symbols

β	volumetric coefficient of thermal expansion $(-1/\rho(\partial\rho/\partial T)_{p,C})$ (K^{-1})
β^*	volumetric coefficient of expansion with mass fraction $(-1/\rho(\partial\rho/\partial C)_{p,T})$
λ	thermal conductivity of the fluid (W m^{-1} K^{-1})
μ	dynamic viscosity of the fluid (kg m^{-1} s^{-1})
ρ	density of the fluid (kg m^{-3})

Subscripts

1	at wet plate
2	at dry plate
0	at ambient conditions

highly affected by the length of the dry zone. A detailed numerical analysis for interfacial heat and mass transfer in air over a falling liquid film with some experimental measurement was performed by Tsay et al. [9]. Their results show that the cooling of liquid film mainly caused by latent heat transfer is connected with the vaporisation of the liquid film. Tsay et al. [9] mentioned that a flow reversal may results in certain parts of the flow when the inlet temperature of the liquid is much higher than the ambient temperature.

Recognizing a relatively little research on internal flow systems, Chang et al. [10] performed an analysis to investigate the effects of the coupled thermal and mass diffusion on the steady development of the velocity, temperature and concentration fields in the natural convection flow of an air–water vapour mixture in a finite vertical tube. Particular attention was paid to study the heat transfer enhancement through mass diffusion when buoyancy forces are in the same direction and the reduction of heat transfer when they are in the opposite direction [10].

The case of developing free convection in a vertical channel with a reversing buoyancy force has been studied by Lee et al. [11]. The plates of the channel were maintained at uniform surface temperature, higher than the ambient while a heavy gas was transpired through the porous plate. The obtained results illustrate the effects of the opposing buoyancy forces on the axial velocity profiles. A close agreement between the measurement profiles of temperature and concentration with the theoretical predictions was shown. Yan and Lin [12] presented a numerical analysis to investigate the effects of latent heat transfer, in association with the evaporation of a finite liquid film on the channel wall, on the free convective heat and mass transfer. The influences of the system temperature and liquid flow rate on the momentum, heat and mass transfer in both the liquid film and the gas stream are studied in detail. Yan and Lin [12] observed that the

assumption of an extremely thin film thickness is a limiting condition and valid only for the system with a small liquid mass flow rate.

The effects of radiation heat transfer in channels have been widely studied especially for forced convection without mass transfer. Some of these studies have been concerned with fluids, which participate in the radiation process [14,15]. The earlier studies dealt with radiatively non-participating fluid [16–18]. Liu and Sparrow [17] conducted a theoretical study to determine the effect of the plates radiation regarded as black bodies on the convective heating of the fluid which considered to be as non-participating medium. One wall of the channel is heated and the other is insulated. They found that radiant interchange causes the task of convective heating to be shared between two walls. The interaction of natural convection with thermal radiation of gray surfaces in a square enclosed filled with air has been numerically investigated by Akiyama and Chong [22]. All walls are assumed to be gray diffuse emitters and reflectors radiation. It was found that the presence of surface radiation change the average convection Nusselt number and the value of the average radiative Nusselt number rises quickly with the increase of emissivity.

From this literature review, it can be concluded that due to the complexity of couplings between the momentum, heat and mass transfer in the flow, using different simplifying assumptions carried out the early theoretical studies. These assumptions can be summarised in the following:

- The liquid film is assumed to be extremely thin. Under this assumption, transport in the liquid film can be replaced by approximate boundary conditions for gas flow.
- The boundary layer type approximations are generally used. Thus the situations where flow reversal occurs were not investigated in details. A more complicated elliptic flow analysis must be performed [13].
- The use of the Boussinesq approximation (constant thermo-physical properties except for density in the buoyancy term and linearization of buoyancy force variations with temperature and concentration) is common. When the system operates at high temperatures, this assumption becomes inappropriate [10]. It is also important to consider these conditions of radiation heat transfer.
- One can note that the thermal boundary conditions generally are considered to be those of isothermal wall conditions [11,12]. Only a few studies were concerned with the problem of combined heat and mass transfer inside plates, where the channel walls are maintained at prescribed heat fluxes.
- The effects of some independent parameters on heat and mass transfer characteristics are investigated by different authors, such as flow liquid rate, wall temperature, and ambient temperature. Others are briefly or not studied like the ambient pressure conditions, the radiative behaviour of the plates.

2. Analysis

The present investigation deals with a numerical study of combined heat and mass transfer by natural convection induced by two buoyancy forces in a finite vertical channel, in which convective and radiative heat transfer interact. The studied channel is made up of two parallel plates symmetrically heated with uniform density fluxes. The first plate ($y = 0$) is wetted by an extremely thin water film so that it can be regarded as a boundary condition for heat and mass transfer [9]. The second one ($y = 2d$) is dry (Fig. 1). For a given heat flux the moist air in the ambient is drawn in to the channel by the resultant forces of thermal buoyancy and solutal buoyancy. Since the temperature of dry wall is higher than that of air, the buoyancy forces near this surface acts upwards and the gas flow moves in this direction. For air inside humid wall, because temperature distribution along the wall is unknown, the forecast of flow direction is quite complex and will depend on the wall and ambient conditions. For a larger imposed heat flux, the wetted wall temperature is also higher than that in ambient and the fluid at the

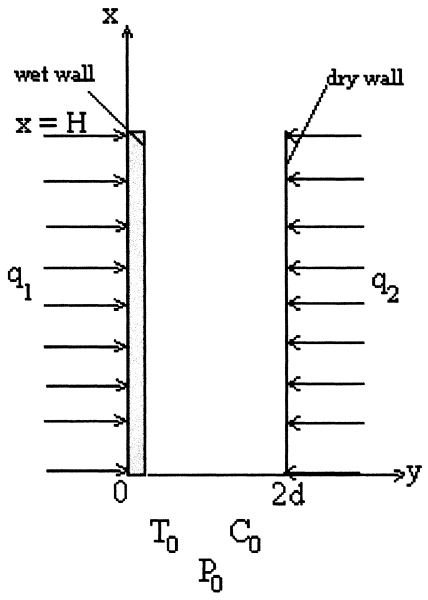

Fig. 1. Schematic view of the physical system.

interface, will move upwards as mentioned in [12], whereas for a smaller heat flux, the water evaporation absorbs a significant amount of energy through latent heat transport. A part of this energy is generated by the heating source. The other part supplied by gas flow through the loss of sensible heat and causes the cooling of the fluid inside the wall. In this case the thermal buoyancy force will act downwards and reduce the velocity field near the interface. For a smaller heating flux and higher ambient temperature a reversal flow can be produced near the humid wall. In this condition we need to solve the full Navier–Stokes equation to know the velocity field in the channel.

In this study, only the case where the resultant of buoyancy forces acts in the upward direction, is treated. The induced flow in the channel is considered to be as a steady two-dimensional flow. The laminar boundary layer approximations are taken into account. The density in the buoyancy force is assumed to be as a linear function with the temperature and the concentration. The thermal conductivity, the dynamic viscosity and the mass diffusivity are taken as variables [9]. The thermo-diffusion and diffusion-thermo effects are neglected.

For radiative transfer, the following assumptions are taken into consideration:

- Air is regarded as a non-participating fluid. This assumption is valid for the present case of small vapour concentration.
- Plates are considered to be opaque, gray, diffuse emitters and diffuse reflectors and have uniform emissivity e.
- Both extremities are assumed to be black bodies at the ambient temperature T_0.

The heat and mass transfer caused by combined buoyancy effects can be described from the following governing equations [24,25]:

Continuity equation

$$\frac{\partial \rho u}{\partial x}+\frac{\partial \rho v}{\partial y}=0 \tag{1}$$

x-Momentum equation

$$u\frac{\partial u}{\partial x}+v\frac{\partial u}{\partial y} =-\frac{1}{\rho}\frac{\mathrm{d}P}{\mathrm{d}x}+\beta g(T-T_0)+\beta^* g(C-C_0) +\left(\frac{1}{\rho}\right)\frac{\partial}{\partial y}\left(\mu\frac{\partial u}{\partial y}\right) \tag{2}$$

$\beta g(T-T_0)+\beta^* g(C-C_0)$ represents the momentum transfer caused by the combined buoyancy forces.

Energy equation

$$u\frac{\partial T}{\partial x}+v\frac{\partial T}{\partial y} =\frac{1}{\rho c_{\mathrm{p}}}\left[\frac{\partial}{\partial y}\left(\lambda\frac{\partial T}{\partial y}\right)+\rho D(c_{\mathrm{pv}}-c_{\mathrm{pa}})\frac{\partial T}{\partial y}\frac{\partial C}{\partial y}\right] \tag{3}$$

In this equation, the viscous dissipation and the pressure work are neglected. The second term in the right side presents the energy transport through the inter-diffusion of species.

Species diffusion equation

$$u\frac{\partial C}{\partial x}+v\frac{\partial C}{\partial y}=\frac{1}{\rho}\frac{\partial}{\partial y}\left(\rho D\frac{\partial C}{\partial y}\right) \tag{4}$$

Another constraint, which is the overall mass balance equation, should be satisfied at every axial location:

$$\int_0^{2d}\rho u(x,y)\mathrm{d}y=2d\rho_0 u_0+\int_0^x \rho v(x,0)\mathrm{d}x \tag{5}$$

Boundary conditions

$$\text{At } x=0;\quad u=u_0,\quad P=-\frac{1}{2}\rho u_0^2,\quad T=T_0,\quad C=C_0 \tag{6}$$

At $x=H$: $P=0$

At $y=0$: $u=0$

- the transverse velocity of gas is deduced by assuming that the air–water interface is semi-permeable:

$$v(x,0)=\frac{-D}{1-C(x,0)}\left.\frac{\partial C}{\partial y}\right|_{y=0} \tag{7a}$$

- the energy balance at the interface ($y=0$) is evaluated by the equation:

$$q=-\lambda\frac{\partial T}{\partial y}-\frac{\rho L_{\mathrm{v}} D}{1-C(x,0)}\frac{\partial C}{\partial y}+q_{\mathrm{rl}} \tag{7b}$$

- Assuming the interface to be at thermodynamic equilibrium and the air–vapour mixture is an ideal gas mixture, the concentration of vapour can be evaluated by:

$$C(x,0)=\frac{M_{\mathrm{v}}/M_{\mathrm{a}}}{p/p_{\mathrm{vs}}+M_{\mathrm{v}}/M_{\mathrm{a}}-1} \tag{7c}$$

p_{vs} is the equilibrium pressure of vapour given by the following equation [6]:

$$\log_{10} p_{\mathrm{vs}}=28.59051-8.2\log T+2.4804\times 10^{-3}T-\frac{3142.32}{T} \tag{7d}$$

At $y = 2d$:

- $u = 0$, $v = 0$;
- the energy balance at this interface is given by:

$$q = \lambda \frac{\partial T}{\partial y} + q_{r2} \tag{7e}$$

- the impermeability of the dry plate ($y = 2d$) to the water vapour can be described by the equation:

$$\frac{\partial C}{\partial y} = 0 \tag{7f}$$

The net radiative fluxes along the plates are [20]:

$$q_{r1}(x_1) = \frac{e}{1-e}(\sigma T^4(x_1) - q_o(x_1)), \tag{8a}$$

$$q_{r2}(x_2) = \frac{e}{1-e}(\sigma T^4(x_2) - q_o(x_2)) \tag{8b}$$

where, q_o (x_1) and q_o (x_2) are the radiosities of the plates at the positions x_1 and x_2:

$$q_o(x_1) = e\sigma T^4(x_1) + (1-e) \times \left\{ \int_{x_2=0}^{x_2=H} q_o(x_2) \mathrm{d}F_{x_1 \to x_2} + F_{x_1 \to O_1} q_o(O_1) + F_{x_1 \to O_2} q_o(O_2) \right\} \tag{8c}$$

$$q_o(x_2) = e\sigma T^4(x_2) + (1-e) \times \left\{ \int_{x_1=0}^{x_1=H} q_o(x_1) \mathrm{d}F_{x_2 \to x_1} + F_{x_2 \to O_1} q_o(O_1) + F_{x_2 \to O_2} q_o(O_2) \right\} \tag{8d}$$

The diffuse view factors $F_{x_1 \to x_2}$ (fraction of radiation leaving the infinitesimal segment dx_2 at the position x_2 of the dry wall and arrives at the subsurface $\mathrm{d}x_1$ of the humid plate) and $F_{x_2 \to x_1}$ (defined between the segment x_1 of the humid wall and $\mathrm{d}x_2$ of the opposite plate) are expressed as following [20]:

$$\mathrm{d}F_{x_1 \to x_2} = \frac{1}{2} \frac{(2d)^2}{((x_2 - x_1)^2 + (2d)^2)^{3/2}} \mathrm{d}x_2 \tag{8e}$$

$$\mathrm{d}F_{x_2 \to x_1} = \frac{1}{2} \frac{(2d)^2}{((x_1 - x_2)^2 + (2d)^2)^{3/2}} \mathrm{d}x_1 \tag{8f}$$

View factors between the segment $\mathrm{d}x_1$ and the aperture O_1 or O_2 are obtained by using the reciprocity relation and the conservation of radiative energy leaving $\mathrm{d}x_1$:

$$2\mathrm{d}F_{O_1 \to x_1} = \mathrm{d}x_1 F_{x_1 \to O_1} \text{ and } 2\mathrm{d}F_{O_2 \to x_1} = \mathrm{d}x_1 F_{x_1 \to O_2} \tag{8g}$$

$$F_{O_1 \to x_1} + F_{O_2 \to x_1} + \int_{x_2=0}^{x_2=H} \mathrm{d}F_{x_2 \to x_1} = 1 \tag{8h}$$

View factors between $\mathrm{d}x_2$ and apertures are expressed in a similar way.

Energy transport between the channel wall and moist air depends on different factors such as the fluid temperature gradient at the walls, the rate of mass transfer and plates radiative properties. The relative importance of energy transport through these different factors can by evaluated along wetted wall by local dimensionless heat transfer rates given by the following ratios:

$$\text{for latent heat:} \quad \frac{q_l}{q_1} = -\frac{1}{q_1}\left(\frac{\rho D L_v}{1 - C(x,0)} \left.\frac{\partial C}{\partial y}\right|_{y=0} \right) \tag{9a}$$

$$\text{for sensible heat:} \quad \frac{q_{s1}}{q_1} = -\frac{\lambda}{q_1} \left.\frac{\partial T}{\partial y}\right|_{y=0} \tag{9b}$$

$$\text{for radiative heat transfer:} \quad \frac{q_{r1}(x_1)}{q_1} \tag{9c}$$

The interfacial evaporating rate is expressed as:

$$\dot{m}(x) = \int_0^x \rho v(x,0) \mathrm{d}x \tag{10a}$$

The local dimensionless wall shear stress is given by:

$$\tau = \mu_0 \frac{\left.\partial u/\partial y\right|_{y=0}}{0.5\rho_0 u_0^2} \tag{10b}$$

3. Solution method

The governing equations were solved numerically by using a finite difference marching procedure in the downstream direction with a regular grid point. The axial convection terms were approximated by the upstream difference and the transverse convection, and diffusion terms by the central difference.

For a given thermal and mass boundary conditions, the resolution procedure is described as follows:

1. Guess the inlet velocity u_0.

2. For the given axial location i, guess the wetted wall temperature: $T(i, 1)$ and solve the finite difference form of species equation for $j = 1$ to J.
3. Solve the finite difference form of energy equation for $j = 1$ to J, then compare the new value of temperature $T^*(i, 1)$ to $T(i, 1)$ by testing if:

$$\left|\frac{T(i,1) - T^*(i,1)}{T(i,1)}\right| < 10^{-6}$$

If this criterion is not satisfied, return to Eq. (2) and modify the wetted wall temperature by using the bisection method.
4. Guess a pressure $P(i)$ at the i axial location and solve the momentum and continuity finite difference equations.
5. Check the satisfaction of the overall conservation of mass expressed by the following criteria:

$$\frac{\left|\int_0^{2d} \rho u(x,y)\mathrm{d}y - (2d\rho_0 u_0 + \int_0^x \rho v(x,0)\mathrm{d}x)\right|}{(2d\rho_0 u_0)} < 10^{-6}$$

If this condition is not satisfied, return to Eq. (4) and modify the pressure value $P(i)$.
6. Repeat the procedure (Eqs. (2)–(5)) for $i = 2$ to $i = I$.
7. Solve the integral equations (Eqs. (8c) and (8d)) to determine the radiosity functions $q_o(x_1)$ and $q_o(x_2)$ using the iterative method of Gauss Seidel. Then determine the net radiative heat fluxes over the surface of plates $q_{r1}(x_1)$ and $q_{r2}(x_2)$ from Eqs. (8a) and (8b).
8. Check the satisfaction of the interfacial heat balance expressed as follows:

for the humid plate:

$$\left|\left[q_1 - (q_{r1} + q_{s1} + q_{l1})\right]/q_1\right| < 10^{-4}$$

for the dry plate: $\left|\left[q_2 - (q_{r2} + q_{s2})\right]/q_2\right| < 10^{-4}$

else, return to Eq. (2) and use the new values of radiative heat fluxes.
9. Test if the exit dynamic pressure is zero, else return to Eq. (1) and modify the inlet velocity by using bisection method.

Since the temperature distributions along the two plates are unknown in Eq. (3), q_{r1} and q_{r2} are taken to be zero at the first iteration. Further, the effect of radiative transfer is taken into consideration by using temperature values obtained in the last iteration.

Several grid sizes are tested and comparison of the results among the computations is given in Table 1. Significant difference in evaporating mass flow ($\dot{m}(x = H)$) is noted by using 30×20 and 70×70 grids. However, comparing the results from a 100×100 grid with 70×70 grid shows a good agreement for all quantities (within 2.5%). As a result 70×70 grid is retained to study the heat and mass characteristics.

Table 1
The total evaporative rate and interfacial Nussel number at the exit for various grid arrangement ($T_0 = 293$, $q_1 = q_2 = 100$, $w = 100\%$, $p_0 = 1$, $d/H = 0.05$)

$I \times J$ grid point	$\dot{m}(H)$	$Nus\,(H)$
30×20	2.490×10^{-5}	106.96
70×50	2.682×10^{-5}	106.69
70×70	2.70×10^{-5}	106.03
100×100	2.734×10^{-5}	105.49

4. Results and discussion

To verify the numerical scheme outlined above, the results for the case of natural convection induced by thermal buoyancy forces with the two cases of constant and variable physical properties were first obtained. The procedure have been tested by comparing the present results of Nusselt number to those found in Thomas [21] and Vachon [6] for the problem of free convection from a flat plate subject to a uniform flux. The comparison is carried out in the case of

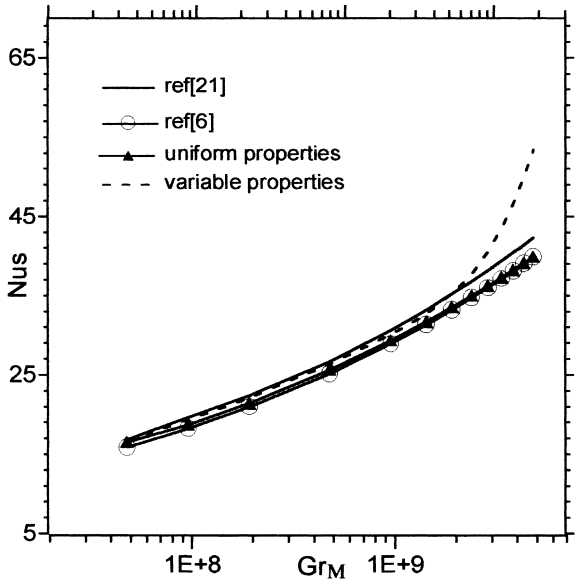

Fig. 2. Variation of the local Nusselt number at the exit of the channel with the Grashof number for the case of pure free convection.

a great channel depth, where the heat transfer is similar to the case of two independent walls [3]. The results of this first comparison presented in Fig. 2 show a good agreement especially for small Grashof numbers. However, for higher Grashof numbers, a slight difference is noted between the different results when the variability of the thermophysical properties is taken into account.

For mass transfer at the humid channel wall, the comparison between our results obtained for a larger channel width and those of Vachon [6] for the free convection from a vertical humid flat plate gives a good agreement as observed in Table 2. The latter gives the evaporating mass flow rates at the channel exit for different parameters.

Furthermore, the numerical code has been tested successfully by comparing the present solutions for temperature profiles with the results of Yahyaoui [19] for the case of natural convection induced by thermal buoyancy with radiative surface effects.

The first section of this study is carried out in order to investigate the effect of wall and ambient conditions on the development of velocity, temperature and concentration profiles as well as on the characteristics of heat and mass transfer. The effect of plate radiation on interfacial heat and mass transfer is studied in the second part.

4.1. Development of the flow, thermal and mass fields

In order to understand the development of the natural convective flow driven by temperature and concentration gradients and the effects of the prescribed heat flux and the ambient parameters, different profiles of temperature, velocity and concentration are presented in Figs. 3–6 for the case of negligible radiative transfer.

The development of axial velocity in the channel is plotted in the Fig. 3a. It is shown that the velocity profiles of air stream develop gradually from uniform distribution at the inlet to destroyed ones as flow goes upstream and keep decreasing the channel at centre. For the case of $q = 500$ (Fig. 3a), the maximum velocity is obtained near plates where the combined buoyancy forces are more pronounced especially near dried wall. This fact, added to the overall mass balance, justify why velocity decreases at the centre line in the streamwise direction.

In Fig. 3c, temperature distribution is given for different axial locations. These profiles show a development of two thermal boundary layers with smaller temperature obtained near the humid wall ($y = 0$), where the heating flux contribute to liquid evaporation which serves as a heat barrier. Concentration profiles are presented in Fig. 3e, which indicate a rapid development of mass boundary layer. These curves show that the water vapour concentration increases gradually as the flow moves in the channel.

The inspection of temperature profiles corresponding to a smaller heating flux (Fig. 3d), shows that the gas flow near the humid plate is cooled especially at the channel inlet due to the fact that the energy needed to water evaporation is higher than that given by the heating source. The excess of energy is supplied by the gas flow through the loss of sensible heat. Therefore the cold fluid near the humid plate slows down (Fig. 3b).

The thermal field is clearly influenced by the ambient temperature variation (Fig. 4) especially for humid plate side. It observed the occurrence of cooling of the fluid near the humid wall. This can be understood by realising that the water evaporation serves as a heat barrier, which is more important for higher T_0.

The effect of the ambient pressure on the development of the axial velocity, temperature and concentration profiles is shown in Fig. 5. It is clearly seen that, when P_0 decreases, the axial velocity at the channel entrance increases (Fig. 5a) and an important cooling of the humid air near the wet plate is observed (Fig. 5b). However, for the dry plate ($y = 2d$), it is shown that the lower pressure gives a higher fluid temperature and by the way, increases the driving force due to the heat transfer (Fig. 5a).

As the air moves in the channel, the mass fraction

Table 2
Variation of the total evaporative rate for various conditions ($p_0 = 1$, $d/H = 0.05$)

T_0 (°C)	$q_1 = q_2$ (W m^{-2})	w (%)	Variable properties	Uniform properties	Vachon [6]
10	100	20	2.30×10^{-5}	3.05×10^{-5}	3.04×10^{-5}
10	100	40	2.51×10^{-5}	2.92×10^{-5}	2.92×10^{-5}
20	100	100	2.70×10^{-5}	2.95×10^{-5}	2.99×10^{-5}
30	100	20	3.77×10^{-5}	4.18×10^{-5}	3.91×10^{-5}
30	250	20	8.40×10^{-5}	9.33×10^{-5}	9.42×10^{-5}
20	400	20	1.22×10^{-4}	1.35×10^{-4}	1.35×10^{-4}
20	400	80	1.18×10^{-4}	1.31×10^{-4}	1.31×10^{-4}

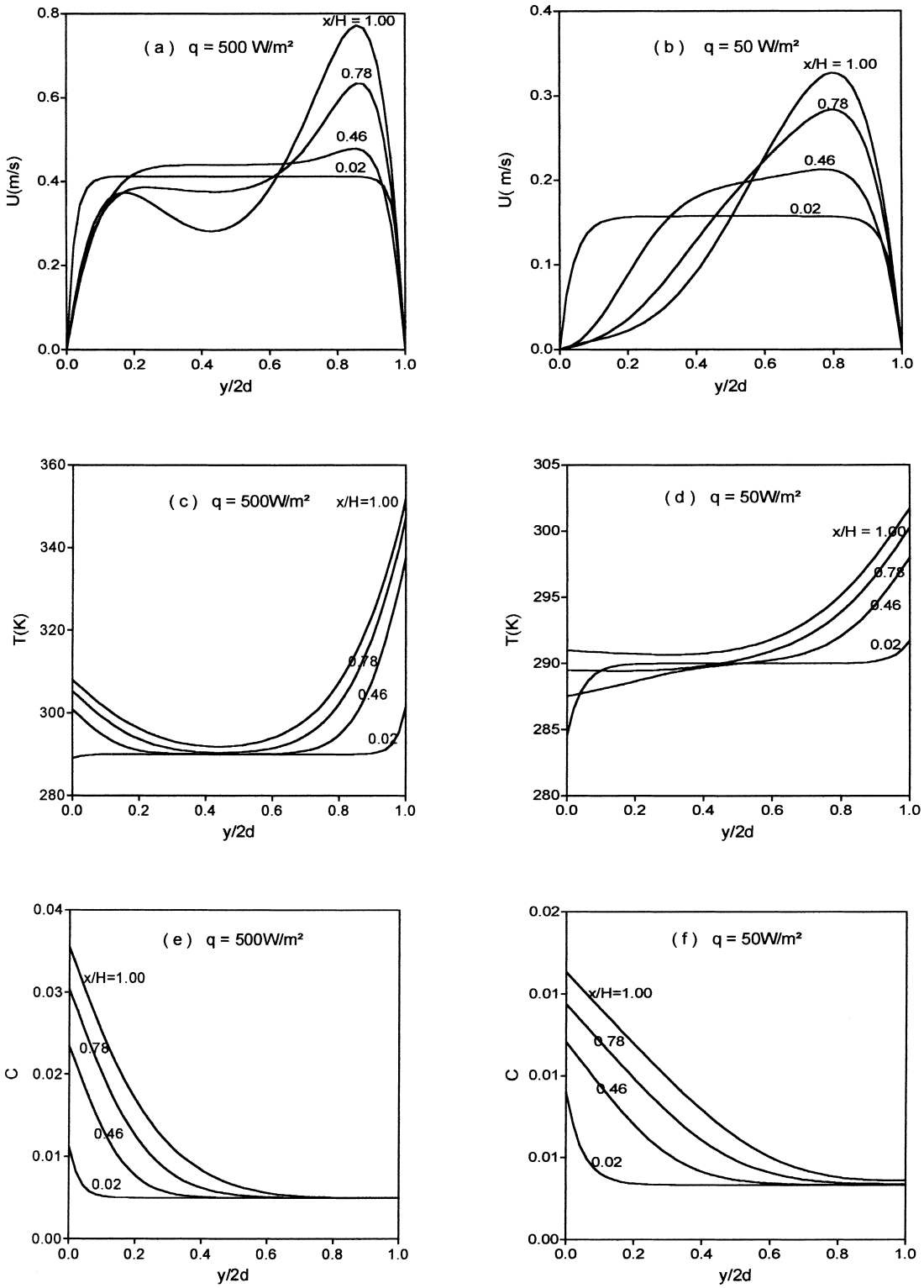

Fig. 3. Effects of the heat flux on the temperature, velocity and concentration profiles ($T_0 = 290$, $C_0 = 0.005$, $p_0 = 1.015$, $d/H = 0.02$).

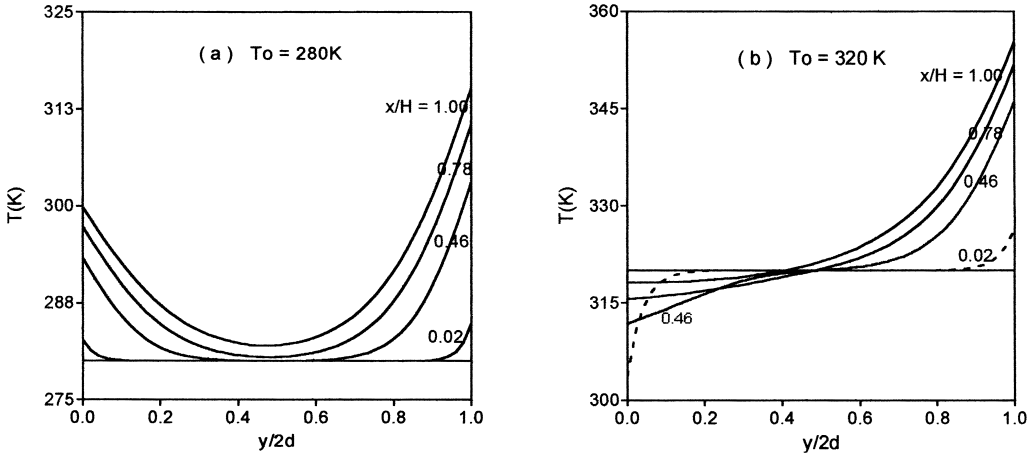

Fig. 4. Effects of the ambient temperature on the temperature profiles ($C_0 = 0.005$, $p_0 = 1$, $d/H = 0.02$, $q = 200$).

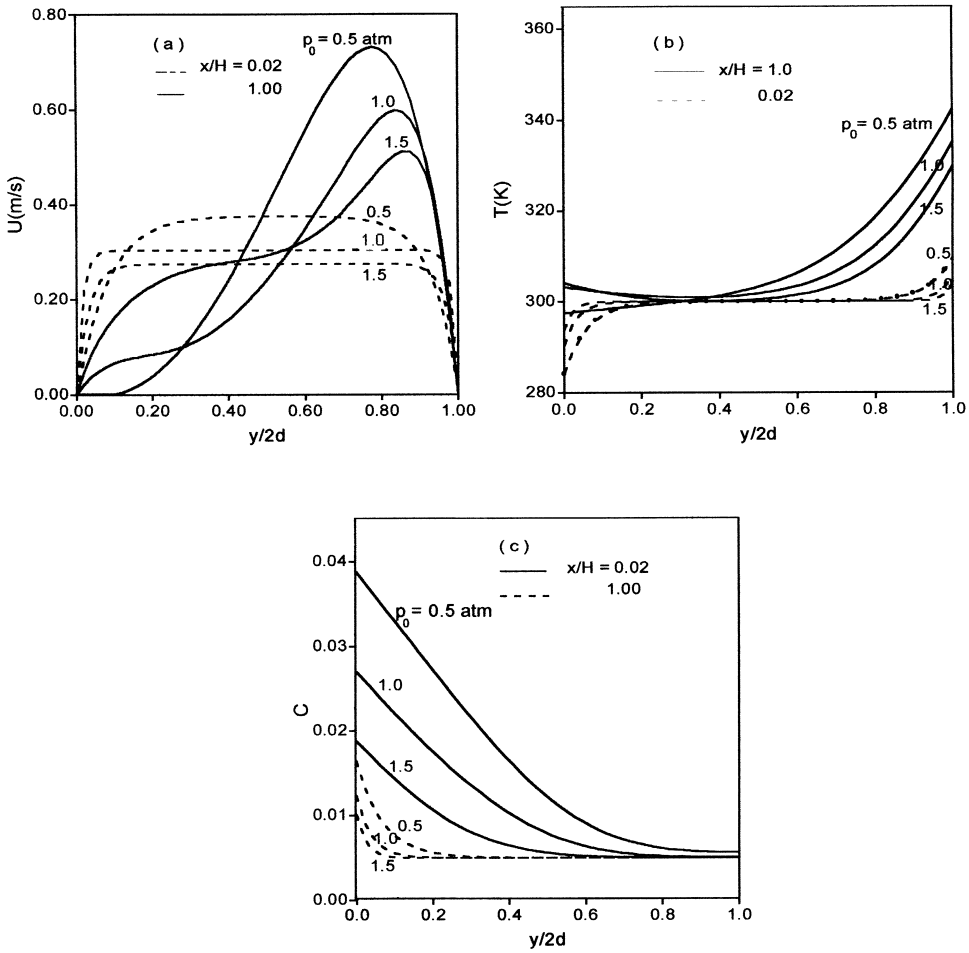

Fig. 5. Effects of the ambient pressure on the flow, concentration and temperature fields ($C_0 = 0.005$, $T_0 = 300$, $d/H = 0.02$, $q = 200$).

of water vapour shown in Fig. 5c increases because of the evaporation of water in the air stream. It can be noted that, for a fixed axial position and if the ambient pressure P_0 goes lower, the concentration goes higher. This increase can be justified from Eq. (7c) where a higher concentration exists at the interface for lower P_0.

Fig. 6 illustrate the changing behaviours of velocity, temperature and concentration fields with a variation of the channel width. Fig. 6a shows that at the channel entrance ($x/H = 0.02$), the axial velocity remains almost uniform for different values of d/H. Further downstream, the buoyancy effects become significant and perturb considerably the flow field. The evaporative cooling (Fig. 6b) reduces the velocity of the humid air adjacent to the wet wall. We can note a striking change in the velocity profiles with the increase of d/H. Velocity profile exhibits two local maximum near the walls, while in the central region, the flow is considerably reduced and becomes stagnant for higher values of d/H.

From results given in Fig. 6 and for a higher channel depth, three regions can be identified. First is the central one where the flow is almost stagnant. In second and third regions, adjacent to the walls, boundary layer profiles of temperature and velocity are observed. It is important to note that these profiles are similar to those of a vertical heated plate [5,6].

4.2. Distributions of the interfacial heat and mass fluxes

To investigate the relative importance of the sensible heat and latent heat exchange along the humid plate, Fig. 7a gives the heat transfer rates (q_{s1}/q_1) and (q_l/q_1)

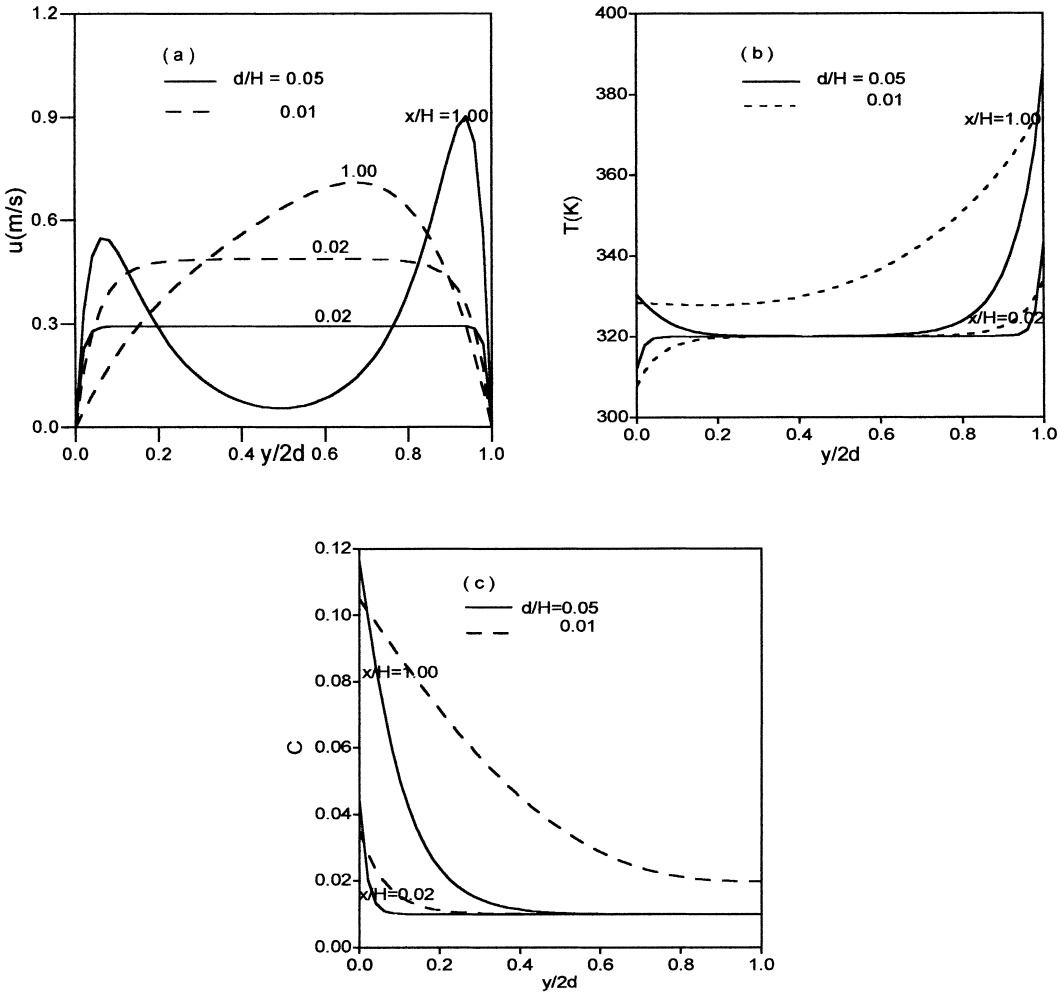

Fig. 6. Effect of the channel width on the velocity, temperature and concentration profiles ($C_0 = 0.005$, $T_0 = 320$, $q = 200$, $p_0 = 1$, $d/H = 0.02$).

along the interface. It can be noted that (q_{s1}/q_1) increases toward the flow direction and reaches a constant value near the channel exit. An opposite trend is shown for (q_l/q_1) in order to respect the energy balance at the interface. As predicted from temperature profiles presented in Fig. 3d and Fig. 7a show that for smaller heating flux the sensible heat transfer at the inlet region is towards the interface. This result, which indicates for smaller fluxes, cooling of interface at the inlet can occurs, is in line with the above discussion. For latent heat rate, it can be noted that q_l/q_1 is always positive, because only the case of evaporation is treated. Fig. 7a also shows that most part of the imposed flux serves in water vaporisation. Thus, heat transfer at the interface is dominated by the transport of latent heat in association with the water vaporisation. Similar conclusions are observed by Chang et al. [9]. The effect of imposed heat flux q $(q=q_1+q_2)$ on mass transfer across the interface is illustrated in Fig. 7b. As seen before for concentration profiles the interfacial evaporating rate $\dot{m}(x)$ increases when the heating flux goes higher.

The heat and mass transfer at the humid plate depends also on the ambient concentration of water vapour C_0 as seen in Fig. 8. These curves show that the latent heat transfer is relatively effective for a smaller C_0. This trend results from the fact that mass diffusion at the interface becomes more important when C_0 decreases and added to the interfacial energy balance, which leads to a drop in the sensible heat transfer. Cooling of the interface at the channel inlet can occur for smaller C_0. As seen in Fig. 8b, a decreasing in the ambient humidity increases the interfacial mass flux.

Fig. 9 shows the axial development of the reduced wall shear stress for different values of the inlet concentration. One can identify two different regions. In a short region near the channel entrance, τ decreases with the axial coordinate as dictated by the development of the hydrodynamic boundary layer. On the other hand, natural convection effects tend to increase the friction. These opposing effects may result in the existence of a local minimum of τ. The presence of latent heat transfer induces a deceleration of the fluid adjacent to the wet plate and hence causes a reduction of wall shear stress. It is observed that an augmentation of C_0 induces an increasing of τ at the wet wall side (Fig. 9). For a small value of C_0 ($C_0=0.001$), the wall shear stress is very small indicating that the fluid velocity approaches zero. This fact results from the important reduction of sensible heat flux at the humid plate.

Fig. 10 presents the interfacial mass flux at the channel exit $\dot{m}(x=H)$ as the function of inlet temperature T_0 for various ambient humidity and pressure. It is clearly observed that the interfacial mass rate increases with an increase in inlet temperature or a decrease in ambient pressure. Further, it is seen that for a smaller temperature system T_0 and a higher value of P_0 an increase in C_0 leads to a drop on the evaporative rate. However for a higher temperature, a reversal trend is observed for a lower P_0, where the evaporating mass flux is less important for smaller humidity values.

It is important to mention that in the case of forced convection with evaporation, the existence of the inversion temperature is well known. Hasan et al. [23] in their study of the laminar evaporation from flat surfaces into unsaturated and superheated solvent vapour, reported that below a certain temperature of the free stream (defined as the inversion temperature), the evaporation rate declines as the stream humidity rises.

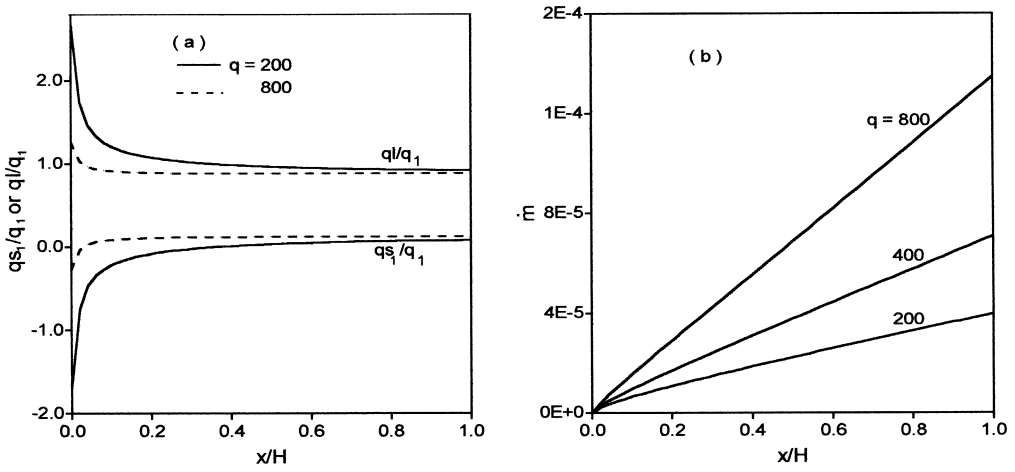

Fig. 7. Effect of heating flux on the interfacial heat fluxes and the evaporating mass flow ($C_0=0.005$, $T_0=300$, $p_0=1$, $d/H=0.02$).

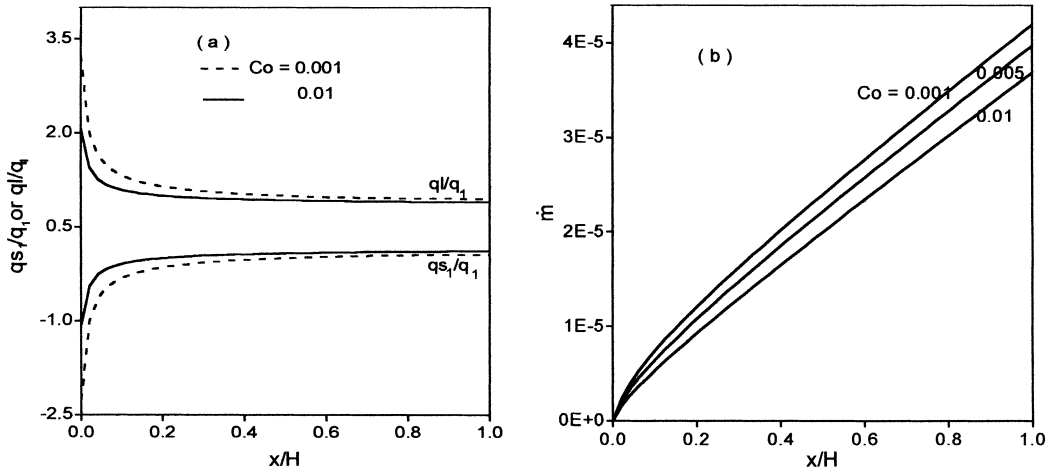

Fig. 8. Effect of the inlet concentration C_0 on the interfacial heat fluxes and evaporating mass flow ($T_0 = 300$, $q = 200$, $p_0 = 1$, $d/H = 0.02$).

Beyond the inversion temperature, the evaporation rate enhances as the humidity of air increases.

4.3. Effect of plates radiation

In this section the effects of radiative transfer between plates are taken into consideration. The surfaces of the channel are considered to be gray and with the same emissivity varying from $e = 0$, which means there is no radiation heat exchange between the plates and $e = 1$, which means that the plates are assumed to be black. To compare the results with and without radiation, some plots containing results where radiation is suppressed are presented.

Effect of plates radiation on the interfacial temperature for the wet and dry walls is given in Fig. 11a. The examination of these curves reveals a significant difference between the results with and without radiation. It can be noted that radiation reduces the temperature of the dry plate and increases that of the moist wall. In fact, radiation will deliver energy from the hot plate ($y = 2d$) to other cooled plate ($y = 0$). As verified by Liu and Sparrow [17] for the forced convection problem, radiative transfer tends to bring the temperature of the plates together. Careful observation of curves in Fig. 11a shows a small drop of the interfacial temperature at the channel exit. This can be justified by a rise

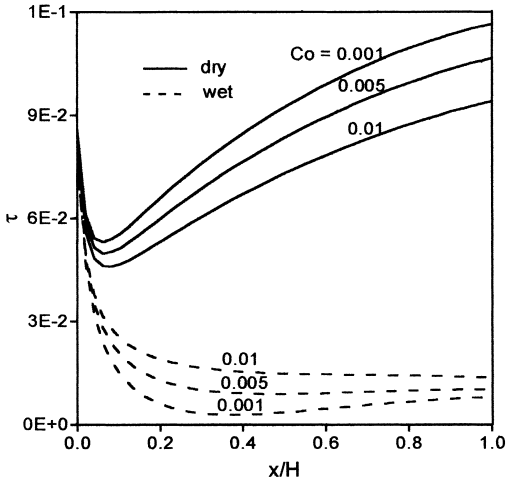

Fig. 9. Axial variation of the wall shear stress for different inlet concentrations C_0 ($T_0 = 300$, $q = 200$, $p_0 = 1$, $d/H = 0.02$).

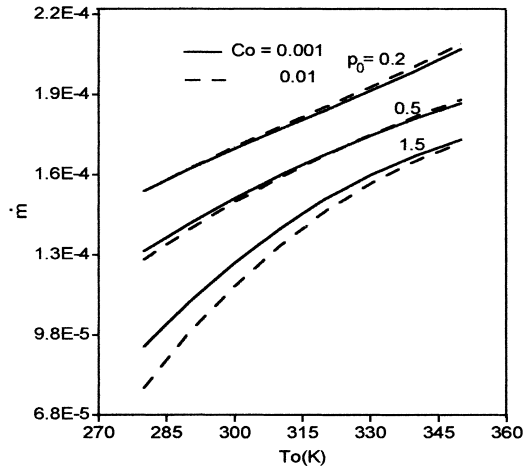

Fig. 10. Effect of the ambient temperature on the evaporation rate ($q = 800$, $d/H = 0.02$).

in radiative flux through exit plenum. Fig. 11a also shows that an increase in plates emissivity intensify the radiation heat exchanged between walls. Whereas, radiative transfer can be neglected for plates with small emissivity. As a result of the increasing temperature of the wet plate, the vapour concentration becomes more important at air–liquid interface as seen in Fig. 11c. Consequently, the thermal and solutal buoyancy forces near the wetted wall become more important and lead to an increase in the streamwise velocity (Fig. 11b). However, the decreasing of the dry wall temperature reduces the thermal buoyancy force and decreases the axial velocity as shown in Fig. 11b.

To provide further perspectives about the role of radiation, distributions of the local heat fluxes on both humid and dry walls are presented in Fig. 12. The ordinate is the ratio of the local sensible, latent or radiative flux to the externally applied flux.

In Fig. 12a the relative sensible, latent and radiative heat fluxes at humid wall are given. Comparison of corresponding curves shows that the magnitude of latent heat transfer q_l/q_1 is much larger than that of sensible and radiative heat fluxes. This result indicates that heat transfer resulting from latent heat exchange is more effective. Because of the decreasing of the radiative energy received by the wet wall at the exit, a small drop in sensible and latent heat is noted.

Fig. 12b shows the distribution of the radiative heat exchange for two different depth values and with an emissivity equal to 0.5. As was discussed earlier in Fig. 11a, the radiative energy transferred in the channel is received by humid plate and loosed by the dry

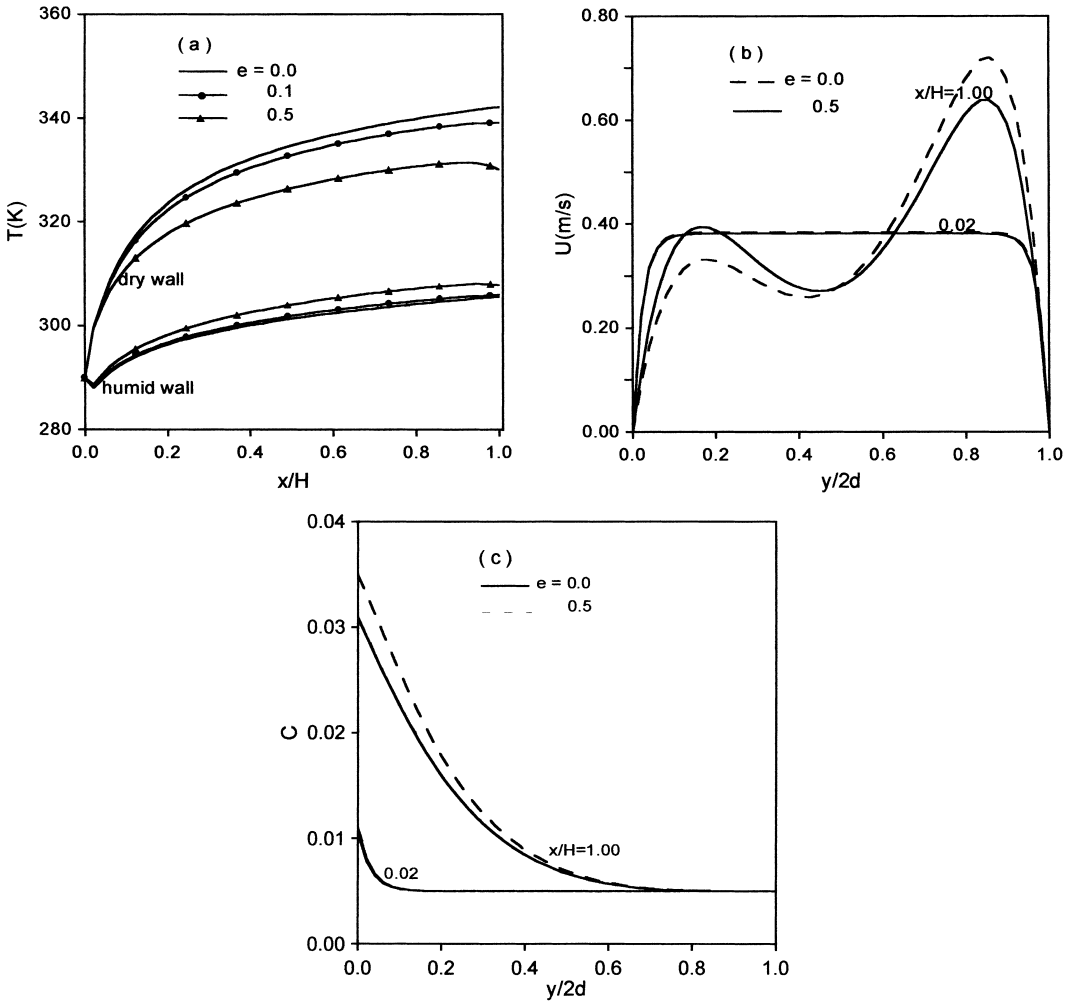

Fig. 11. Effect of plates emissivity on the wall temperature, velocity and concentration profiles ($C_0 = 0.005$, $T_0 = 290$, $q = 400$, $d/H = 0.02$, $p_0 = 1$).

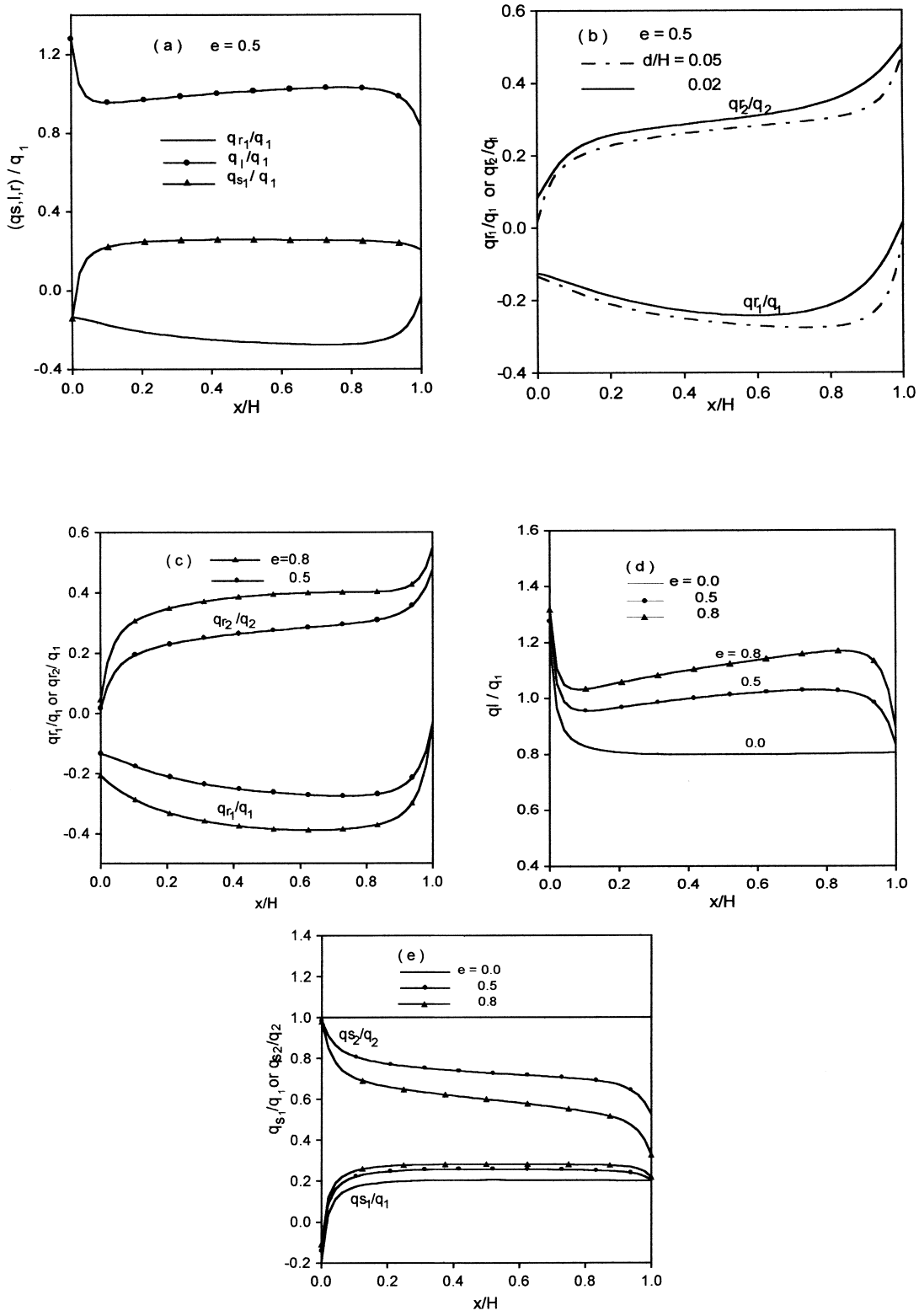

Fig. 12. Distribution of the interfacial heat transfer fluxes along dry and wet plates ($C_0 = 0.005$, $T_0 = 290$, $q = 400$, $d/H = 0.02$, $p_0 = 1$).

one. Near the entrance, lower radiative fluxes are observed because of the smaller wall temperature values. At the exit, the most part of the radiative heat energy transferred in the channel leaves the duct through the opening. Consequently, an important increase in the net radiative energy emitted by the dry wall is observed, and a drop in the fraction of radiative energy reaching the humid plate is then noted. From Fig. 12b, it is also noted that an increasing value of d/H leads to a decrease in both q_{r1} and q_{r2}. This result can be explained by a rise in the radiative energy leaving the channel through the opening.

Effect on latent heat transfer due to the variation of emissivity is shown in Fig. 12d. A larger q_l is noted for the plate with higher emisivities. This outcome apparently is due to the higher interfacial radiative flux reaching the wet plate as clearly seen in Fig. 12c, also shows that the increase in e affects the shape of the interfacial latent heat flux. Particularly an important drop-off near the leading edge occurs at higher e, which is caused by the pronounced exit effects.

Local relative heat fluxes for sensible transfer at the dry wall are plotted in Fig. 12e. For dry plate, initially $q_{s2}/q_2 \approx 1$, and then decreases with increasing x, rather rapidly at first and then more gradually. Near the exit, a sharp drop is noted. This result indicates that heat transfer at this interface is dominated by convection in particular near the inlet because of the relative high heat transfer associated with the initial thermal development of the flow. It is important to mention that Liu and Sparrow [17] obtained similar results for the problem of combined internal convection and radiation with one heated plate and the other is adiabatic.

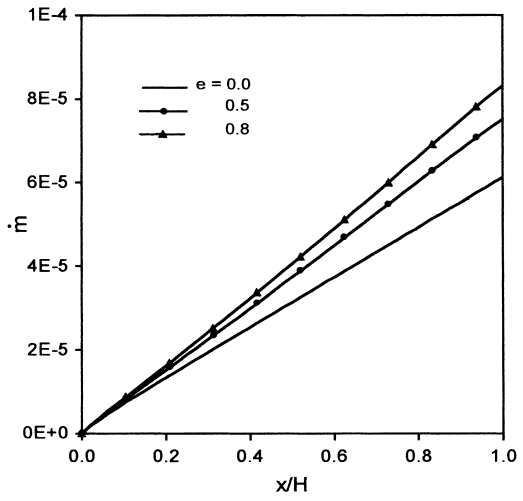

Fig. 13. Effect of the plates emissivity on the interfacial mass transfer rate ($C_0=0.005$, $T_0=290$, $q = 400$, $d/H = 0.02$, $p_0=1$).

According to the larger radiative heat flux leaving the dry wall for higher emissivity (Fig. 12c), an important decrease in sensible heat flux occurs for this plate. Whereas for the wet one, sensible heat is slightly increased owing to water evaporation which absorbs the greater amount of energy delivered by radiation as discussed in Fig. 12d.

The influence of radiation on the evaporating rate along the wetted interface is presented in Fig. 13. A rise in the magnitude of $\dot{m}(x)$ results a higher emissivity. This behaviour is consistent with the already discussed fact that radiation deliver more energy at high emissivity. Owing to this result, the optimal case for water evaporation takes place when the plates participate as black bodies.

5. Concluding remarks

The natural convection flow resulting from the combined thermal and solutal buoyancy effects in a vertical channel has been numerically studied for an air–water system. The effects of the prescribed heat flux, the ambient temperature, concentration and pressure on the characteristics of the heat and mass transfer are examined in detail. The radiative transfer between plates was also to be considered.

The major results are briefly summarised in the following:

- The evaporative cooling at the wet interface disturbs considerably the velocity and temperature profiles in particular near the exit section of the channel.
- A decreasing of the applied heat flux induce an important cooling of the fluid adjacent to the wet wall. A situation with a reversal flow in this region may occur for smaller values of the prescribed heat flux.
- The interfacial heat and mass transfer at humid plate is dominated by the water vaporisation. However, the dry wall convection plays an important role in the heat transfer process.
- Plates with higher emissivity increase the amount of evaporated water. Thus, it can be said that the optimum case of evaporation occurs when channel surfaces are black.

References

[1] W. Aung, G. Worku, Developing flow and flow reversal in a vertical channel with asymmetric wall temperatures, ASME J. Heat Transfer 108 (1986) 299–304.

[2] W. Aung, G. Worku, Theory of fully developed combined convection including flow reversal, ASME J. Heat Transfer 108 (1986) 485–488.

[3] A.M. Dalbert, F. Penot, J.L. Peube, Convection naturelle laminaire dans un canal vertical chauffé à flux constant, Int. J. Heat Mass Transfer 24 (9) (1981) 1463–1473.
[4] C. Prakash, Y.D. Liu, Buoyancy induced flow in a vertical internally finned circular duct, ASME J. Heat Transfer 107 (1985) 118–123.
[5] B. Gebhart, L. Pera, The nature of vertical natural convection flows resulting from combined buoyancy effects of thermal and mass diffusion, Int. J. Heat Mass Transfer 14 (1971) 2025–2050.
[6] M. Vachon, Etude de l'évaporation en convection naturelle, Thèse de doctorat, Université de Poitiers, 1979.
[7] W.M. Yan, C.Y. Soong, Convective heat and mass transfer along an inclined heated plate with film evaporation, Int. J. Heat Mass Transfer 38 (7) (1995) 1261–1269.
[8] M. Mammou, M. Daguenet, G. Le Palec, Numerical study of heat and mass transfer from an inclined flat plate with wet and dry zones, Int. J. Heat Mass Transfer 35 (9) (1992) 2277–2287.
[9] Y.L. Tsay, T.F. Lin, W.M. Yan, Cooling of a falling liquid film through interfacial heat and mass transfer, Int. J. Multiphase Flow 16 (5) (1990) 853–865.
[10] C.J. Chang, T.F. Lin, W.M. Yan, Natural convection flows in a vertical open tube resulting from combined buoyancy effects of thermal and mass diffusion, Int. J. Heat Mass Transfer 29 (10) (1986) 1543–1552.
[11] T.S. Lee, P.G. Parikh, A. Acrivos, D. Bershader, Natural convection in a vertical channel with opposing buoyancy forces, Int. J. Heat Mass Transfer 25 (4) (1982) 499–511.
[12] W.M. Yan, T.F. Lin, Combined heat and mass transfer in natural convection between vertical parallel plates with film evaporation, Int. J. Heat Mass Transfer 33 (3) (1990) 529–541.
[13] K.T. Lee, H.L. Tsay, W.M. Yan, Mixed convection heat and mass transfer in a vertical rectangular ducts, Int. J. Heat Mass Transfer 40 (7) (1997) 1621–1631.
[14] A. Soufiani, J. Taine, Application of statistical narrow-band model to coupled radiation and convection at high temperature, Int. J. Heat Mass Transfer 30 (1987) 437–447.
[15] Y. Kurosaki, Radiation heat transfer in a flow between parallel flat plates with temperature slips at walls, Fifth International Heat Transfer Conference 1 (1974) 98–102.
[16] J.R. Carpenter, D.G. Briggs, V. Sernas, Combined radiation and developing laminar free convection between vertical flat plates with asymmetric heating, ASME J. Heat Transfer 104 (1976) 501–507.
[17] C.H. Liu, E.M. Sparrow, Convective radiative interaction in a parallel plate channel — application to air-operated solar collectors, Int. J. Heat Mass Transfer 23 (1980) 1137–1146.
[18] E.M. Sparrow, W.Q. Taw, Buoyancy driven fluid flow and heat transfer in a pair of interacting vertical parallel channels, Numerical Heat Transfer 5 (1982) 39–58.
[19] M. El Yahyaoui, Influence des effets radiatifs et conductifs sur la convection naturelle entre deux plaques planes verticales parallèles chauffées à flux constants, thèse de troisième cycle, Université de Poitiers, 1983.
[20] N.M. Ozisik, Radiative Transfer and Interactions with Conduction and Convection, Wiley, New York, 1973, p. 574.
[21] L.C. Thomas, Heat Transfer, Prentice-Hall, New Jersey, USA, 1992.
[22] M. Akiyama, Q.P. Chong, Numerical analysis of natural convection with surface radiation in a square enclosure, Numerical Heat Transfer, Part A 31 (1997) 419–433.
[23] M. Hasan, A.S. Mujumdar, M. Al Taleb, Laminar evaporation from flat surfaces into unsaturated and superheated solvent vapor, drying 1986, Hemisphere (1986) 604–616.
[24] M.W. Kays, M.E. Crawford, Convective Heat and Mass Transfer, McGraw-Hill, New York, 1980.
[25] H. Schlichting, Boundary Layer Theory, McGraw-Hill, New York, 1979.